Supporting Information: Tunable phonon-induced transparency in bilayer graphene nanoribbons

Hugen Yan[1†*], Tony Low[1†*], Francisco Guinea[2], Fengnian Xia[1] and Phaedon Avouris[1*]

[1] *IBM T.J. Watson Research Center, Yorktown Heights, NY 10598, USA*

[2] *Instituto de Ciencia de Materiales de Madrid. CSIC. Sor Juana Inés de la Cruz 3. 28049 Madrid, Spain*

† *These authors contributed equally to the work.*

∗ *hyan@us.ibm.com, talow@us.ibm.com, avouris@us.ibm.com*

(Dated: April 2, 2014)

I. BILAYER GRAPHENE HAMILTONIAN

We consider a bilayer graphene arranged in the Bernal stacking order with basis atoms A_1, B_1 and A_2, B_2 in the top and bottom layers respectively. The intralayer coupling is γ_0 and the interlayer coupling between A_2 and B_1 is γ_1. The non-interacting electronic Hamiltonian in the (A_1, B_1, A_2, B_2) basis representation in the vicinity of **K** valley reads[1],

$$\mathcal{H}_0 = \sum_{\mathbf{k}} \hat{a}^\dagger_{\mathbf{k}} H_{\mathbf{k}} \hat{a}_{\mathbf{k}} \tag{1}$$

with

$$H_{\mathbf{k}} = \begin{bmatrix} \Delta/2 & v_F\pi_- & 0 & 0 \\ v_F\pi_+ & \Delta/2 & \gamma_1 & 0 \\ 0 & \gamma_1 & -\Delta/2 & v_F\pi_- \\ 0 & 0 & v_F\pi_+ & -\Delta/2 \end{bmatrix} \tag{2}$$

where $\pi_\pm = \hbar(k_x \pm \mathrm{i}\, k_y)$, $v_F = {}^3L_2\gamma_0/\hbar$, L is the carbon-carbon bondlength and Δ is the on-site energy difference between the two layers. The electronic bands and wavefunctions are obtained by diagonalizing $H_{\mathbf{k}}$. The electronic bands are denoted by $\xi_n(\mathbf{k})$, with $n = 1, 2, 3, 4$ in ascending energy order given by,

$$\xi_n(\mathbf{k}) = \pm\frac{1}{2}\sqrt{\pm 2\Omega + \Delta^2 + 2\gamma_1^2 + 4v_F^2\pi_+\pi_-} \tag{3}$$

where $\Omega \equiv \sqrt{4\Delta^2 v_F^2\pi_+\pi_- + 4v_F^2\gamma_1^2\pi_+\pi_- + \gamma_1^4}$ and the signs are chosen as $-+$, $--$, $+-$ and $++$ for $n = 1, 2, 3, 4$ respectively. Their 4-component wavefunctions denoted by $|\Phi_n(\mathbf{k})\rangle$ are given by,

$$\frac{1}{N}\begin{bmatrix} 1 \\ \frac{1}{2v_F\pi_-}(2\xi_n - \Delta) \\ \frac{1}{2v_F\gamma_1\pi_-}(-2\Delta\xi_n + \Delta^2 + \gamma_1^2 \pm \Omega) \\ \frac{1}{8v_F^2\gamma_1\pi_-^2}(-4\Delta v_F^2\pi_-\pi_+ - 8\xi_n\pi_+\pi_- v_F^2 - 8\xi_n\gamma_1^2 + \Delta^3 + 4\gamma_1^2\Delta + 8\xi_n^3 - 4\xi_n^2\Delta - 2\xi_n\Delta^2) \end{bmatrix} \tag{4}$$

where N is the normalization constant, and the $\pm$ sign are choosen as $+$, $-$, $-$ and $+$ for $n = 1, 2, 3, 4$ respectively.

II. ELECTRON PHONON HAMILTONIAN

The only intrinsic phonons with momenta and energies similar to the graphene plasmons in our experiment are the long wavelength longitudinal/transverse optical (LO/TO) phonons near the Γ point, with energies $\hbar\omega_{op} \approx 0.2\,\mathrm{eV}$. The relative displacement of the two sublattice in top layer is given by

$$\mathbf{u}_T(\mathbf{r}) = \mathbf{u}(\mathbf{r}) = \sqrt{\frac{\hbar}{2\rho_m\omega_{op}A}}\sum_{\mathbf{p}\lambda}(\hat{b}_{\mathbf{p}\lambda} + \hat{b}^{\dagger}_{\text{-}\mathbf{p}\lambda})\mathbf{e}_\lambda(\mathbf{p})e^{i\mathbf{p}\cdot\mathbf{r}} \tag{5}$$

where ρ_m is the mass density of graphene, $\mathbf{p} = (p_x, p_y)$ is the phonon wavevector, λ denotes the LO/TO modes, $\hat{b}^{\dagger}_{\mathbf{p}\lambda}$ and $\hat{b}_{\mathbf{p}\lambda}$ are the creation and destruction operators, $\mathbf{e}_\lambda(\mathbf{p})$ are the polarization vectors given by $\mathbf{e}_{LO}(\mathbf{p}) = i(\cos\varphi, \sin\varphi)$ and $\mathbf{e}_{TO}(\mathbf{p}) = i(-\sin\varphi, \cos\varphi)$ where $\varphi = \tan^{-1}(p_y/p_x)$. Due to the two graphene layers, there are two possible vibrational modes i.e. symmetric ($\mathbf{u}_B(\mathbf{r}) = \mathbf{u}(\mathbf{r})$) and antisymmetric mode ($\mathbf{u}_B(\mathbf{r}) = -\mathbf{u}(\mathbf{r})$).

The electron-phonon coupling at the **K** valley for bilayer graphene is given by[2],

$$H_{e-op}(\mathbf{r}) = -\sqrt{2}\frac{\beta\hbar v_F}{L^2}\boldsymbol{\sigma}^{\pm} \times \mathbf{u}(\mathbf{r}) \tag{6}$$

with $\sigma_j^+ = I\sigma_j$ and $\sigma_j^- = \sigma_z\sigma_j$ where σ_j are the Pauli matrices and $\beta = -\partial\ln\gamma_0/\partial L$ is a dimensionless parameter related to the deformation potential. Assuming the electric field polarized along y and $\varphi = 0$, we have $\mathbf{e}_{LO}(\mathbf{p}) = (1, 0)$ and $\mathbf{e}_{TO}(\mathbf{p}) = (0, 1)$. Since only lattice vibration along y can couples to light, we consider only the TO mode. As a result, we can write the electron-phonon interaction for the v mode in the following form,

$$\mathcal{H}'_v = \frac{1}{\sqrt{A}}\sum_{\mathbf{k}}\hat{a}^{\dagger}_{\mathbf{k}+\mathbf{p}}\mathcal{V}_v(\mathbf{p})\hat{a}_{\mathbf{k}}e^{i\mathbf{p}\cdot\mathbf{r}}(\hat{b}_{\mathbf{p},v} + \hat{b}^{\dagger}_{\mathbf{p},v}) \tag{7}$$

where $v = A, S$ denotes the symmetric and antisymmetric modes, with

$$\mathcal{V}_S(\mathbf{p}\to 0) = igI\sigma_x \tag{8}$$

$$\mathcal{V}_A(\mathbf{p}\to 0) = ig\sigma_z\sigma_x \tag{9}$$

$$g = \frac{\beta\hbar v_F}{L^2}\sqrt{\frac{\hbar}{2\rho_m\omega_{op}}} \tag{10}$$

where g has the dimension of Jm^{-1} and assumed to be $\approx 0.3\,\mathrm{eV\AA}^{-1}$ in our calculation.

III. DIELECTRIC RESPONSE

The plasmon response of bilayer graphene begins with finding the dielectric function, obtained by adding the various contributions independently as follows,

$$\epsilon_T^{RPA}(q,\omega) = \epsilon_{env} - v_c\Pi^0_{\rho,\rho}(q,\omega) - v_c\frac{q^2}{\omega^2}\delta\Pi_{j,j}(q,\omega) \tag{11}$$

where $v_c = e^2/2q\epsilon_0$, q and ω is the plasmon wave-vector and frequency. $\Pi^0_{\rho,\rho}(q,\omega)$ is the non-interacting part (i.e. the pair bubble diagram) of the charge-charge correlation function given by,

$$\Pi^0_{\rho,\rho}(q,\omega) = -\frac{g_s g_v}{(2\pi)^2}\sum_{nn'}\int d\mathbf{k}\frac{n_F(\xi_n(\mathbf{k})) - n_F(\xi_n(\mathbf{k}+\mathbf{q}))}{\xi_n(\mathbf{k}) - \xi_{n'}(\mathbf{k}+\mathbf{q}) + \hbar\omega + i\hbar/\tau_e}\left|F_{nn'}(\mathbf{k},\mathbf{q})\right|^2 \tag{12}$$

where n_F is the Fermi-Dirac distribution function, $F_{nn'}(\mathbf{k},\mathbf{q})$ is the band overlap,

$$F_{nn'}(\mathbf{k},\mathbf{q}) = \langle\Phi_n(\mathbf{k})\,|\Phi_{n'}(\mathbf{k}+\mathbf{q})\rangle \tag{13}$$

and τ_e is the electron lifetime.

Electron-phonon interaction modifies the current-current correlation function (i.e. optical conductivity) whose contribution we denote by $\delta\Pi_{j,j}(q,\omega)$. We employ a model for $\delta\Pi_{j,j}(q,\omega)$ which is consistent with the various electron-phonon selection rules for the symmetric/antisymmetric modes and Fano effect observed in optical spectroscopy experiments for bilayer graphene and is given by[3],

$$\delta\Pi_{j,j}(q,\omega) = \sum_{vv'}\Gamma_{j,v}(q,\omega)\mathcal{D}_{vv'}(\omega)\Gamma_{v'^\dagger,j}(q,\omega) \tag{14}$$

where

$$\Gamma_{j,v}(q,\omega) = -\frac{g_s g_v}{(2\pi)^2}\sum_{nn'}\int d\mathbf{k}\frac{n_F(\xi_n(\mathbf{k})) - n_F(\xi_n(\mathbf{k}+\mathbf{q}))}{\xi_n(\mathbf{k}) - \xi_{n'}(\mathbf{k}+\mathbf{q}) + \hbar\omega + i\hbar/\tau_e}[\mathcal{J}]_{nn'}[\mathcal{V}_v]_{n'n} \tag{15}$$

$$[\mathcal{J}]_{nn'} = \langle\Phi_n(\mathbf{k})|\,\mathcal{J}\,|\Phi_{n'}(\mathbf{k}+\mathbf{q})\rangle \tag{16}$$

$$[\mathcal{V}_v]_{nn'} = \langle\Phi_n(\mathbf{k})|\,\mathcal{V}_v\,|\Phi_{n'}(\mathbf{k}+\mathbf{q})\rangle \tag{17}$$

with $v = A, S$ and the current operator defined as $\mathcal{J} \equiv v_F I\sigma_y$ with the direction of the electric field. $\mathcal{D}$ is the phonon Green's function defined as,

$$[\mathcal{D}^{-1}(\omega)]_{vv'} = \delta_{vv'}[\mathcal{D}_0^{-1}(\omega)] - \Gamma_{v^\dagger,v'}(\omega) \tag{18}$$

where $\mathcal{D}_0 = 2\omega_{op}/\hbar((\omega + i/\tau_{op})^2 - \omega_{op}^2)$ is the free phonon Green's function and τ_{op} describes the phonon lifetime. In this calculation, we assumed $\tau_{op} \approx 10\,\text{ps}$.

IV. RAMAN SPECTRUM OF BILAYER GRAPHENE

Fig. S1a shows the 2D mode of bilayer graphene nanoribbons. The multiple-component structure of the spectrum has been widely used to identify AB-stacked bilayer graphene[4]. Fig. S1b is the spectrum for the G, D and D' modes. Due to defects introduced by nanoribbon edges, the defect related modes D and D' are quite visible in the spectrum. Similar to the infrared active phonon mode in Fig. 1b of the main text, the Raman active G mode phonon frequency is also around $1580\,\mathrm{cm}^{-1}$.

V. COUPLED OSCILLATOR MODEL FOR THE PLASMON-PHONON COUPLED SYSTEM

The spectrum of bilayer graphene plasmon can be phenomenologically modeled by the power dissipation of two coupled mechanical oscillators[5]. Fig. S2a depicts the coupled oscillators. The equations of motion read:

$$\begin{aligned} \ddot{x}_1 + \gamma_1\dot{x}_1 + \omega^2 x_1 - \Omega^2 x_2 &= \frac{F}{m} exp(-i\omega_s t) \\ \ddot{x}_2 + \gamma_2\dot{x}_2 + (\omega+\delta)^2 x_2 - \Omega^2 x_1 &= 0 \end{aligned} \tag{19}$$

where x_1 and x_2 are the displacements, ω and $\omega+\delta$ are the frequencies of the two oscillators without coupling, γ_1 and γ_2 are the damping rates, ω_s is the driving frequency. $\Omega = \sqrt{\kappa/m}$, with κ as the coupling spring constant. The average power absorbed by oscillator 1 as a function of the driving force frequency can be derived based on Eq. 19 as:

$$P(\omega_s) = \frac{2\pi i F^2 \omega_s[(\omega+\delta)^2 - \omega_s^2 - i\gamma_2\omega_s]}{m[(\omega^2 - \omega_s^2 - i\gamma_1\omega_s)((\omega+\delta)^2 - \omega_s^2 - i\gamma_2\omega_s) - \Omega^4]} \tag{20}$$

We fit the plasmon spectrum in the main text of Fig. S2b using the real part of Eq. 20. The fitting parameters are as follows: the phonon frequency is $1574.6\,\mathrm{cm}^{-1}$, the phonon damping rate is $7.9\,\mathrm{cm}^{-1}$, the plasmon frequency is $1558.7\,\mathrm{cm}^{-1}$, the damping rate is $192.1\,\mathrm{cm}^{-1}$ and the coupling constant $\Omega = 312.3\,\mathrm{cm}^{-1}$.

In order to have a pronounced and well-defined PIT, the coupling constant should have an appropriate value. Fig. S2b shows the simulated spectra with 3 different coupling constants while other crucial parameters such as the phonon and plasmon frequencies and linewidths

are kept the same as the fitting parameters for Fig. 2b in the main text. Its clear that with a small coupling constant, the phonon feature is only a small perturbation to the plasmon spectrum, while a large coupling strength splits the plasmon into two well-separated plasmon modes with similar intensity and linewidth.

VI. PLASMONS IN TRILAYER GRAPHENE NANORIBBONS

We also measured the plasmon spectra in ABA-stacking trilayer graphene nanoribbons. Fig. S3 presents the measured extinction spectra with both parallel and perpendicular light polarization for a trilayer graphene nanoribbon array with ribbon width of 110 nm. The coupling strength between the plasmon and phonon is weaker than in the case of bilayer graphene, because the PIT is not as pronounced. The reason for the weaker coupling requires further theoretical and experimental investigations. Presumably its due to a weaker phonon dipole moment in trilayer graphene.

VII. FANO PARAMETER q_f FOR THE PHONON FEATURE

We extracted the phonon spectra by subtracting the plasmon contribution in the spectra shown in the main text and then fit the spectra with the Fano formula[6],

$$1 - \frac{T}{T_s} = \frac{2p}{\pi\Gamma(q_f^2+1)} \frac{(q_f+\epsilon)^2}{(1+\epsilon^2)} \tag{21}$$

where Γ is the phonon linewidth, p is a parameter for the amplitude, q_f is a parameter accounting for the linseshpae and $\epsilon = 2(\omega - \omega_{ph})/\Gamma$ with ω_{ph} as the phonon frequency. Since the phonon Fano lineshape depends strongly on the plasmon frequency with respect to the phonon frequency, it is informative to plot the Fano parameter q_f as a function of the plasmon frequency detuning for different ribbon widths and different Fermi levels. Fig. S4 plots the extracted q_f as a function of the plasmon frequency detuning with respect to the phonon frequency. It shows that when the plasmon frequency is below the phonon frequency, the parameter q_f is positive, and when the plasmon frequency is higher than the phonon frequency, q_f is negative. Our experiment demonstrates that q_f can be continuously tuned from positive to zero to negative values through either active method such as gating or passive ways such as control of the ribbon width or chemical doping. To understand the

behavior more quantitatively, we adopted a formalism introduced by Li et al.[7] to calculate the Fano parameter q_f:

$$q_f = \frac{1}{\pi} P \int \frac{d\omega}{\omega_{ph} - \omega} \left| \frac{A_{pl}(\omega)}{A_{pl}(\omega_{ph})} \right|^2 \tag{22}$$

where P denotes the principal value of the integral, $A_{pl}(\omega)$ is the optical transition amplitude due to the plasmon absorption. To simulate the results in Fig. S4, we used a Lorentzian with linewidth of 250 cm^{-1} to represent $A_{pl}(\omega)$. By substituting the plasmon absorption spectrum with variable peak frequency into Eq. 22, the parameter q_f can be directly calculated as a function of the plasmon frequency. The solid curve in Fig. S4 is the calculated result which is in reasonable agreement with the experiment.

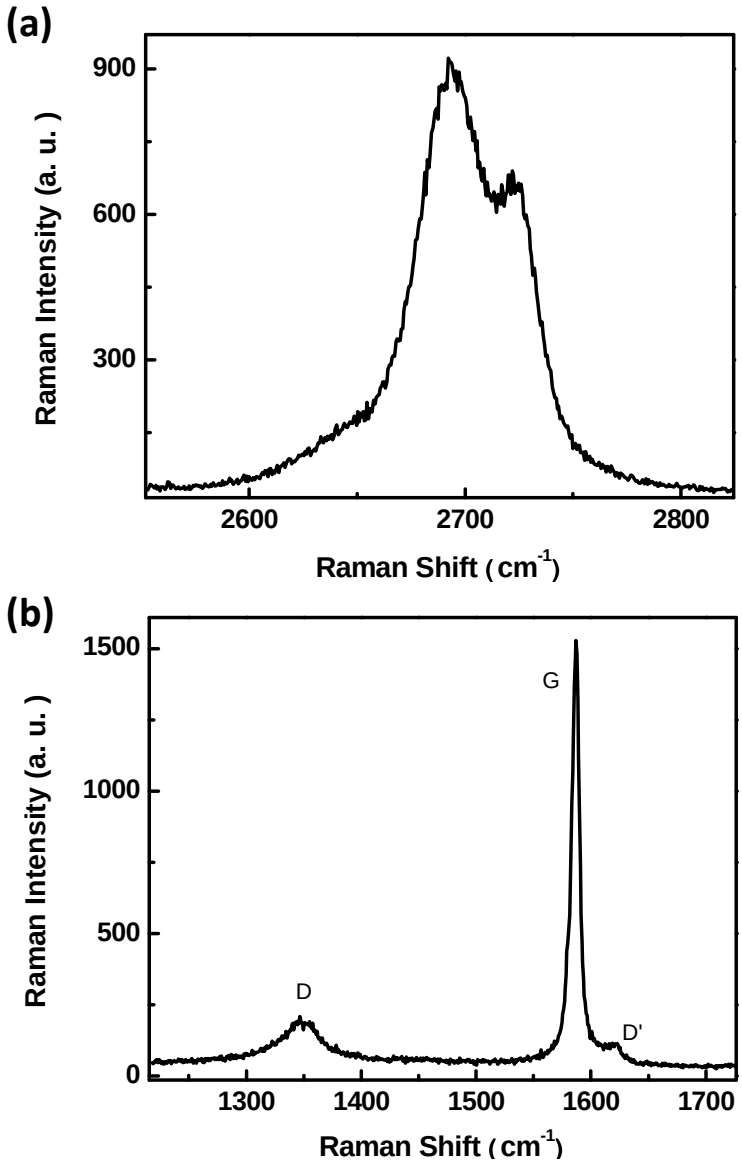

FIG. S 1: **Raman spectra of bilayer graphene nanoribbons.** **(a)** 2D mode and **(b)** G mode, D mode and D' mode.

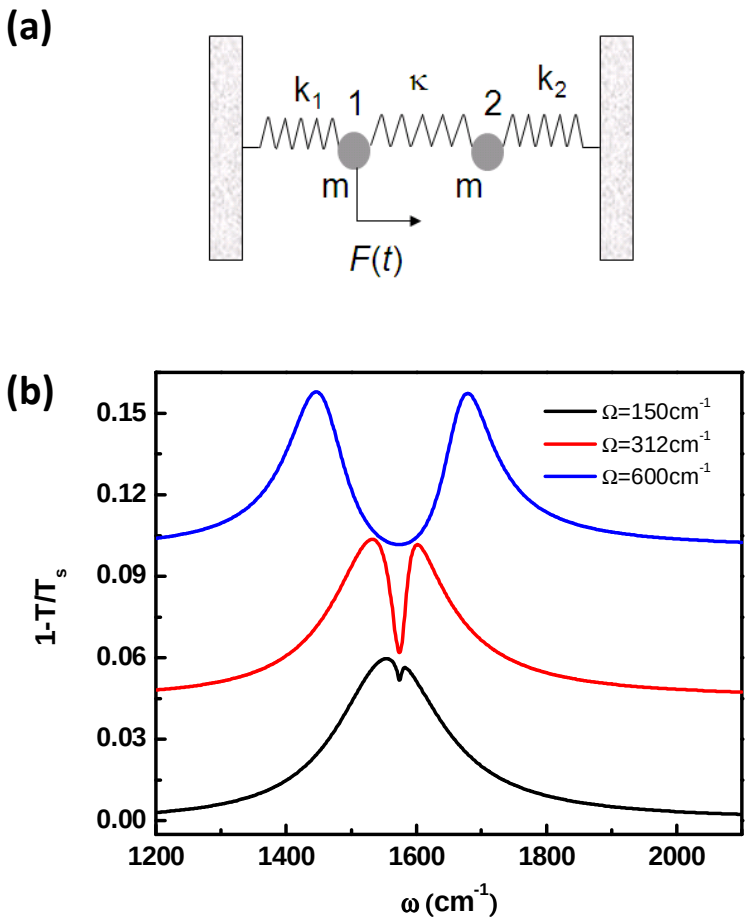

FIG. S 2: **Coupled oscillator model.** **(a)** An illustration of the two coupled mechanical oscillators. k_1, k_2 and κ are spring constants and m is the mass. **(b)** Calculated extinction spectra based on the model with different coupling constants. Only appropriate coupling strength can have well-defined PIT. Spectra are shifted vertically for clarity.

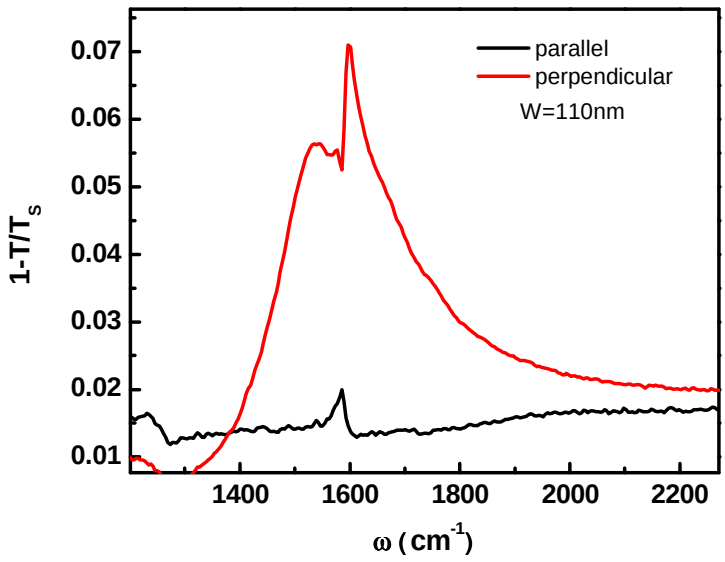

FIG. S 3: **Trilayer graphene nanoribbon spectra.** Extinction spectra for a trilayer graphene nanoribbon array (ribbon width $W = 110\,\mathrm{nm}$) with both parallel and perpendicular light polarizations.

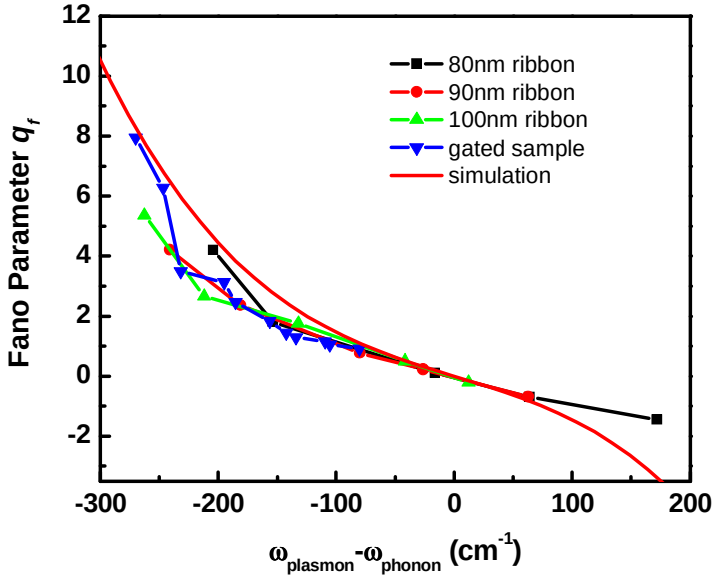

FIG. S 4: **Fano parameter** q_f. q_f dependence on the plasmon frequency detuning with respect to the phonon frequency for 4 different graphene nanoribbon arrays with different widths and Fermi levels. One of the data sets is from a gated sample. The solid curve is the simulated result.

[1] E. McCann, Phys. Rev. B **74**, 161403R (2006).

[2] T. Ando, J. Phys. Soc. Jpn **76**, 104711 (2007).

[3] E. Cappelluti, L. Benfatto, M. Manzardo, and A. B. Kuzmenko, Phys. Rev. B **86**, 115439 (2012).

[4] A. Ferrari, J. Meyer, V. Scardaci, C. Casiraghi, M. Lazzeri, F. Mauri, S. Piscanec, D. Jiang, K. Novoselov, S. Roth, et al., Phys. Rev. Lett. **97**, 187401 (2006).

[5] C. G. Alzar, M. Martinez, and P. Nussenzveig, Am. J. of Phys. **70**, 37 (2002).

[6] U. Fano, Phys. Rev. **124**, 1866 (1961).

[7] Z. Li, C. H. Lui, E. Cappelluti, L. Benfatto, K. F. Mak, G. L. Carr, J. Shan, and T. F. Heinz, Phys. Rev. Lett. **108**, 156801 (2012).